by redesign to eliminate liquid helium. The glass Dewar system is somewhat impractical and might be replaced by a plastic system. Another practical addition to the research effort would be the use of a closed-system helium gas refrigerator. Maximum benefit of such a system would be obtained if materials such as niobium, having higher critical temperatures, are used.

ACKNOWLEDGMENTS

The advice and support of Dr. L. W. Zelby, Director of the school of Electrical Engineering of the University of Oklahoma, is greatefuly acknowledged, as is the able assistance of J. Barrett, O. G. Ramer, C. W. Alworth, and A. A. Kochis.

JOURNAL OF APPLIED PHYSICS VOLUME 40, NUMBER 5 APRIL 1969

Slow-Wave Structures Utilizing Superconducting Thin-Film Transmission Lines*

P. V. MASON

Jet Propulsion Laboratory, California Institute of Technology, Pasadena, California 91103

AND

R. W. GOULD

California Institute of Technology, Pasadena, California 91109

Slow-wave propagation of electromagnetic waves in transmission lines formed of thin-film superconductors has been studied theoretically and experimentally. Previous theoretical analyses have been extended to include nonlocal theories. Strong dependence of phase velocity is found on film thickness and interfilm spacing when these become less than a few penetration depths. Velocity is also modified by coherence length, mean free path, nature of reflection of electrons at the film surfaces, and by temperature and magnetic field. Experimental measurements were made to verify the dependence on thickness, spacing, and temperature by means of a resonance technique. Agreement with theory was excellent in the case of temperature. Data taken for varying thickness and spacing verified the general trend of theoretical predictions. They indicate a nonlocal behavior with some specular reflection, but scatter of the data taken for different films prevents precise comparison of theory and experiment. Estimates of bulk penetration depths were made for indium, $\lambda_{In}=648\pm130$ Å. For tantalum a rough estimate could be made of $\lambda_{Ta}=580$ Å. Data were consistent with the estimate of coherence length for indium of $\xi_0\approx3000$ Å. Velocity was found to be independent of frequency in the range 50–500 MHz, while losses increased as the square. Pulse measurements indicated that delays of several microseconds and storage of several thousand pulses on a single line are feasible.

I. INTRODUCTION

We report in this paper theoretical analysis and experimental measurements of slow-wave propagation on a transmission line formed of thin-film superconductors. We also report some experiments to investigate the suitability of such lines for pulse storage and manipulation.

It was noted by Pippard[1] that the inductive nature of the surface impedance of superconductors would result in an appreciable reduction of the propagation velocity of electromagnetic waves on a line constructed of such materials. He noted that the velocity reduction would be very small for macroscopic conductors, so he proposed and used a technique to measure the small shift of resonant frequency when such a structure undergoes a normal-to-superconducting transition. More recently, Young[2] and co-workers observed that modern thin-film techniques allowed one to form strip transmission lines in which the slowing would be much larger. They observed reductions of about 10%, but were limited by their pulse technique to about 5% accuracy. At about the same time, we reported similar experiments, but used thinner films to obtain much larger reductions, and a resonance technique, which permitted higher accuracy.[3] Alphonse and Bergstein[4] have also reported using the thin-film resonance technique to study the magnetic-field dependence of the Ginsburg–Landau order parameter.

It is of interest to note that the slow-wave mode described here is exactly analogous to a mode existing in a finite plasma, as described by Trivelpiece and Gould,[5] in the case of a London[6] superconductor.

In the next section we analyze the theoretical dependence of velocity on the penetration depths of the superconducting films. We find a linear relationship

* Much of this work was performed at the California Institute of Technology, and was supported by the Office of Naval Research, Washington, D.C. The remainder, which was performed at the Jet Propulsion Laboratory, was supported by the National Aeronautics and Space Administration.

[1] A. B. Pippard, Proc. Roy. Soc. (London) **A191**, 399 (1947).

[2] D. R. Young, J. C. Swihart, S. Tansal, and N. H. Meyers, Bull. Am. Phys. Soc. **5**, 163 (1960).

[3] P. V. Mason and R. W. Gould, Bull. Am. Phys. Soc. **6**, 501 (1961).

[4] G. A. Alphonse and L. Bergstein, Phys. Letters **23**, 221 (1966).

[5] A. W. Trivelpiece and R. W. Gould, J. Appl. Phys. **30**, 1784 (1959).

[6] F. London, *Superfluids* (John Wiley & Sons, Inc., New York, 1950), Vol. I.

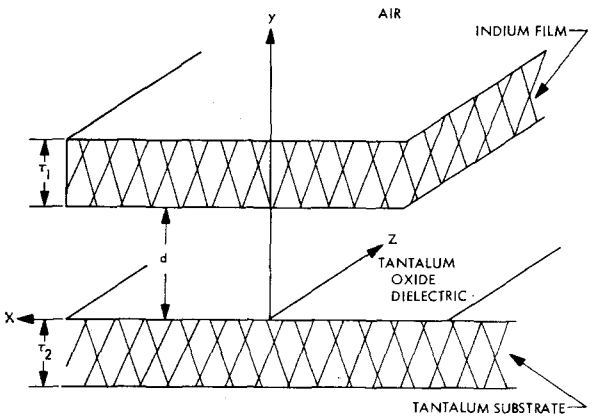

FIG. 1. Geometry of superconducting transmission line.

between inverse velocity squared and the sum of the thickness-dependent penetration depths. We next find the dependence of penetration depth of a film on thickness, bulk penetration depth, coherence length, mean free path, and nature of electron reflection for London and Pippard[7] and Bardeen–Cooper–Schrieffer[8] superconductors.

In the third section, we describe the preparation of the film and the techniques of measurement of velocity and attenuation. In the fourth section, we describe the resonance results and compare them with theory, and present the results of experiments with pulse storage. In the fifth, we summarize our data and give our conclusions.

II. THEORETICAL ANALYSIS

A. General Considerations and Assumptions

Swihart[9] has given a thorough analysis of the velocity dependence on thicknesses and interfilm spacing for a London local superconductor with losses. We have extended this result to include the nonlocal theories of Pippard[7] and Bardeen, Cooper, and Schrieffer.[8] We find it necessary to introduce an assumption about the reflection of superelectrons from the film surfaces, and we present the results for the two extreme cases of completely specular and completely diffuse reflection.

Figure 1 illustrates the transmission line to be analyzed. We assume that the superconductors are characterized by the three bulk parameters: London penetration depth λ_∞, the Pippard coherence length ξ_0, and the coherence length reduced by mean free path effects ξ. As is customary in low-loss transmission lines, we assume that losses introduce an exponential attenuation but do not modify the field distributions. Edge effects are neglected, so that field quantities do not depend on x. The dielectric is assumed lossless, of permeability μ_0, permittivity ϵ_D, and hence supports a plane wave with velocity $c_D=1/(\mu_0\epsilon_D)^{1/2}$. We assume that the propagating mode is an E mode one with velocity appreciably less than c, the free-space velocity of light. TEM modes cannot exist, as noted by Meyers,[10] and H-mode solutions are not slow, and appear to be rapidly attenuated.

We assume a wave traveling in the z direction, so that all field quantities vary as $\exp[j(\omega t-\hat{\beta}z)]$, where the velocity we measure is given by

$$v_\phi=\omega/\beta. \tag{1}$$

B. Relationship between Penetration Depth and Velocity

The quantity measured in the experiments is the phase velocity of an electromagnetic wave; in this section we relate it to the penetration depths of the two superconductors, generalized to include the effect of finite thickness.

The penetration depth, measured at the lower surface, of a film lying in the region $0<y<\tau$ may be defined by

$$\lambda(\tau)=\int_0^\tau H_{\tan}(y)dy/H_{\tan}(0). \tag{2}$$

For an infinitely thick film, $\lambda(\tau)$ reduces to the bulk penetration depth which we will label λ_∞. For a London superconductor, λ_∞ is given by

$$\lambda_\infty=\lambda_L=(m/\mu_0 ne^2)^{1/2}, \tag{3}$$

where m, n, and e are the mass, number density, and charge of the superelectrons.

It is important to note that when one defines $\lambda(\tau)$ by Eq. (2), one must specify the boundary conditions on the far surface of the superconductor. In our analysis of the transmission line, we may assume that the far surface faces a material which is of very high surface impedance, i.e., supports negligible magnetic field. This condition is not met if, e.g., there is another superconductor within a few penetration depths of the far surface. It is also not met in calculations of the magnetic susceptibility of thin superconducting films, such as those of Schrieffer, or Liniger and Odeh,[11] for which the requirement imposed by the experimental conditions is that the magnetic fields on the two sides be equal. Thus, the thickness dependence of penetration depth calculated in this paper differs significantly from that determined from susceptibility calculations.

We show in Appendix A that we can express the phase velocity in terms of the finite-thickness penetration depths λ_1 and λ_2 of the upper and lower films, as measured at their interfaces with the dielectric. The result is

$$(c_D/v_\phi)^2=1+\lambda_1(\tau_1)/d+\lambda_2(\tau_2)/d. \tag{4}$$

[7] A. B. Pippard, Proc. Roy. Soc. (London) **A216**, 547 (1953).
[8] J. Bardeen, L. Cooper, and J. R. Schrieffer, Phys. Rev. **108**, 1175 (1957).
[9] J. C. Swihart, J. Appl. Phys. **32**, 461 (1961).
[10] N. H. Meyers, Proc. IRE **49**, 1640 (1961).
[11] J. R. Schrieffer, Phys. Rev. **106**, 47 (1957); W. Liniger and F. Odeh, Phys. Rev. **132**, 1934 (1963).

Thus we obtain appreciable slowing only if d is small, of the order of a penetration depth. Physical parameters such as temperature, film thicknesses, magnetic field, and frequency enter only as they affect the λ's. In particular, the well-known increase of λ near T_c will cause a large reduction of v_ϕ if d is small. Also, as we shall show, $\lambda(\tau)$ becomes large as τ becomes small, and as the superconducting film is made impure. The velocity change is thus an excellent tool for measuring the effects of these parameters on the superconductors.

The linear dependence of $(c_D/v_\phi)^2$ on the λ's is useful in the analysis of the data. We have no good value for the penetration depth of tantalum. However, in this experiment τ_2 is essentially infinite, and the penetration depth of tantalum varies only a small amount over the temperature range where indium is superconducting. Thus, the variation of $(c_D/v_\phi)^2$ is nearly all due to the indium and only a small correction need be made for the presence of the tantalum in analyzing the temperature dependence. The situation is not as clear cut in the case of the thickness dependence, because a large fixed value for λ_{Ta} enters the equation, masking the dependence on the thickness of the indium film unless the latter is small.

C. Dependence of v_ϕ on Electrodynamics, Surface Reflections, Film Thickness, and Mean Free Path

To calculate the penetration depths we must have a relationship between supercurrent J_s and magnetic vector potential A. This relationship is combined with Maxwell's equations and suitable boundary conditions.

The simplest assumption is the London[6] local case, for which

$$-\mu_0 \mathbf{J}_s(\mathbf{r}) = \mathbf{A}(\mathbf{r})/\lambda_L^2. \tag{5}$$

For the nonlocal Pippard[7] and BCS[8] cases, the J_s–A relationship is more complicated, and we reserve discussion for Appendix B. The two nonlocal cases give nearly identical results, as they should, since the BCS theory is a microscopic justification of the phenomenological Pippard equation.

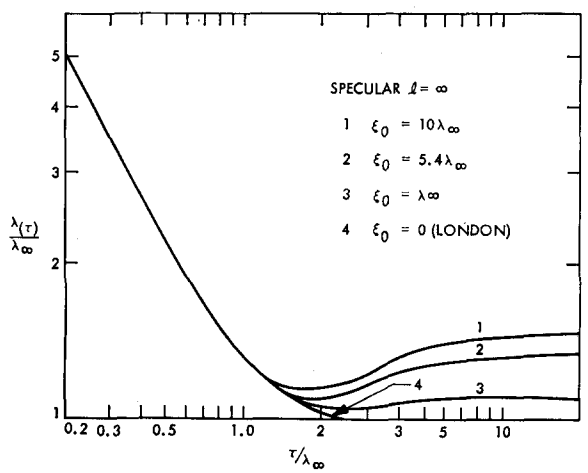

FIG. 2. Theoretical thickness dependence of penetration depth with specular reflection of electrons and infinite mean free path.

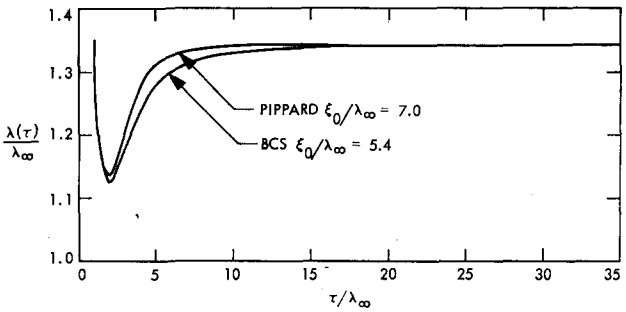

FIG. 3. Comparison of BCS and Pippard penetration depths in the specular case.

We must make an assumption in the nonlocal cases about the reflection of electrons at the film surfaces. We analyze the two extreme cases of complete specular and complete diffuse scattering. Intermediate cases are physically possible, but would be difficult to calculate. The calculations are carried out in Appendix B. The result for the London superconductor is equivalent to that given by Swihart[9]

$$\lambda(\tau) = \lambda_L \coth(\tau/\lambda_L). \tag{6}$$

The case of the pure nonlocal superconductor with specular reflection is analyzed for both the Pippard and BCS theories. In Fig. 2 we show the result for the BCS case with coherence length as a parameter. The curve for $\xi_0=0$ is the London case of Eq. (6). The curve for $\xi_0=5.4\lambda_\infty$ corresponds to Schrieffer's[11] choice for indium, and $\xi_0=10\lambda_\infty$ corresponds to about 3000 Å (assuming that $\lambda_\infty=\lambda_L$), which is in the range given by various investigators, e.g., Toxen.[12]

We see that λ increases very rapidly as the films are made thin (corresponding to a large velocity reduction), and approaches a constant value which depends on ξ_0 as they are made thick. The most striking feature is the minimum at $\tau=2\lambda_\infty$. No minimum was obtained by Schrieffer in his susceptibility calculations. The difference is presumably due to the difference in field and current distributions; in the susceptibility case, for which the external fields are symmetric about the center, interior distributions tend to become uniform, while in the transmission-line case the fields and currents drop to zero at the outer edge. (See, e.g., Fig. 3 of Meyer's paper.[10])

In Fig. 3 we compare the Pippard and BCS results with the ξ_0's chosen to give the same bulk values. The similarity of the BCS and Pippard kernels leads to nearly identical thickness dependences.

The results for the Pippard diffuse case are given in Fig. 4. Note the change in vertical scale. Here we again find a sharp increase in $\lambda(\tau)$ with decreasing τ, and a leveling off to bulk value, but no minimum. In

[12] A. M. Toxen, Phys. Rev. **123**, 442 (1961).

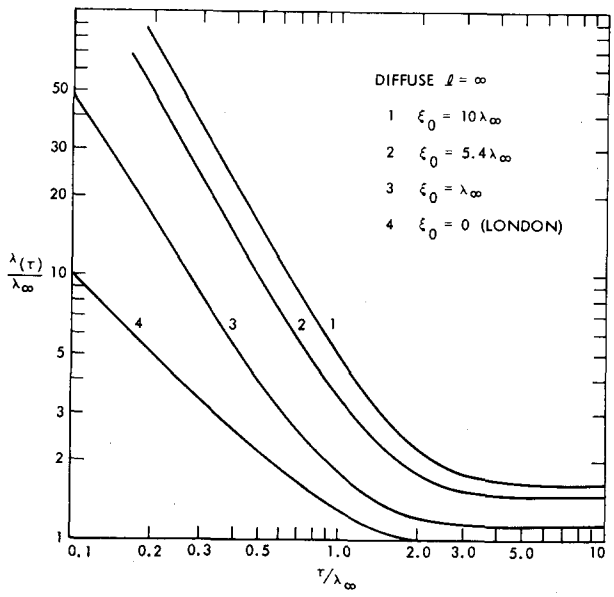

FIG. 4. Theoretical thickness dependence of penetration depth with diffuse reflection of electrons and infinite mean free path.

this case, the small τ values do not tend to the London limit, which is the curve for $\xi_0=0$.

We have not solved the BCS diffuse case, but the similarity of the kernels indicates that the results should be very similar to those of Fig. 4.

We take account of impurity effects by introducing the mean free path l, which may be estimated from the normal-state resistivity by Fuch's relationship.[13] Pippard[7] has proposed that the quantity ξ appearing in his equations be given by

$$\xi^{-1}=\xi_0^{-1}+l^{-1}. \tag{7}$$

Using this equation, we have calculated λ vs t for a number of values of l with $\xi_0=5.4\lambda_\infty$. Results are shown in Fig. 5. λ depends strongly on l, and it appears that an experimental study would be informative. In our experiments, however, we estimate $l>10\lambda_\infty$ and hence need not take account of impurity effects.

It should be remarked that in the theoretical analysis, $\lambda_\infty=(4/3)^{1/2}\lambda_L$ for the BCS case, and $\lambda_\infty=\lambda_L(\xi_0/4\pi\xi)^{1/2}$ for the Pippard case. In fitting the experimental data, however, we have treated λ_∞ as an adjustable parameter.

III. EXPERIMENTAL TECHNIQUES

A. Measurement Technique

A simplified diagram of the measurement apparatus is shown in Fig. 6. The strip transmission line has characteristic impedance Z_1 of a few mΩ, while the signal source, detector and connecting coaxial lines have impedance $Z_0=50$ Ω. Hence, the line acts as a lightly loaded cavity, and appreciable transmission takes place only when the line is an integral number of half-wavelengths long. The velocity is then given by

$$v_\phi=2Lf_n/n, \tag{8}$$

where L is the superconducting line length, f_n is the resonant frequency, and n the mode number. Most measurements were made at the fundamental, which fell between 50 and 300 MHz, but occasionally at higher harmonics up to 500 MHz to study frequency effects.

Signal-generator output power was held at 0.1 mW except in a few cases of high loss. Measurements were not a function of power up to this level.

The sensitivity of the receiver was such that a signal loss of 75 dB through the transmission line could be measured. Loss was measured by replacing the test line by a direct connection, then varying the precision attenuator to give the same reading at the detector. Accuracy was ± 0.2 dB. Frequency was read directly on a counter. Accuracy of frequency determination was at least 0.01%, much better than the frequency stability of the resonant peak, particularly near the critical temperature of indium, where the resonant frequency is a very sensitive function of temperature.

The point of maximum transmission was taken as the resonant frequency. The frequencies of half-power transmission were also measured in order to obtain resonance Q and hence an estimate of the losses on the line itself.

B. Preparation of Sample

The substrate was 0.32 mm, 99.9% pure tantalum sheet produced by Fansteel Metallurgical Co. It was electropolished to remove microscopic roughness, fol-

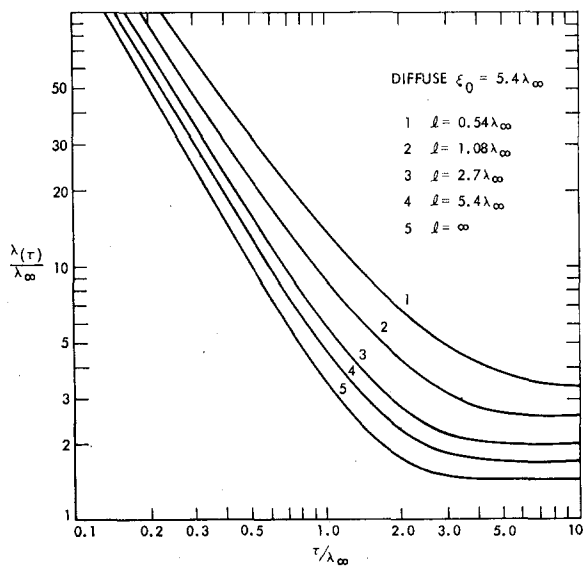

FIG. 5. Theoretical thickness dependence of penetration depth with mean free path as a parameter and fixed coherence length.

[13] K. Fuchs, Proc. Cambridge Phil. Soc. **34**, 100 (1938).

lowing a procedure recommended by Tegart.[14] An insulating layer of Ta_2O_5 of controlled thickness was then formed by anodization in a saturated solution of ammonium borate at room temperature, at a constant current of 2.5 mA/cm² to desired voltage, then at constant voltage until the current dropped to 0.1 mA/cm². This method was used by Charlesby and Polling,[15] who found a voltage–thickness relationship of the form

$$d=d_0+CV. \tag{9}$$

They found $d_0=50$ Å, $C=16.0$ Å/V. Young[16] finds $C=15.1$ Å/V. Other experimenters report varying values for d_0 ranging from 20–50 Å. All agree, however, that the dependence is linear. In any case, the exact value of d is secondary since the most important results can be obtained knowing only that d is constant for a given anodization voltage.

Immediately after anodization, the substrate was cleaned, mechanically and chemically, then placed in an oil-diffusion-pumped, liquid-nitrogen-trapped vacuum-evaporation apparatus. In addition, a Meissner trap was used in the chamber. Pressure measured in the chamber by a nude Baird–Alpert gage was 5×10^{-8} Torr before evaporation, and lower than 10^{-6} Torr during evaporation.

The substrate was held at a temperature of 100°K during indium evaporation to reduce clumping of the indium evaporant, allowing us to make continuous films as thin as 350 Å. Source–substrate distance was 25 cm.

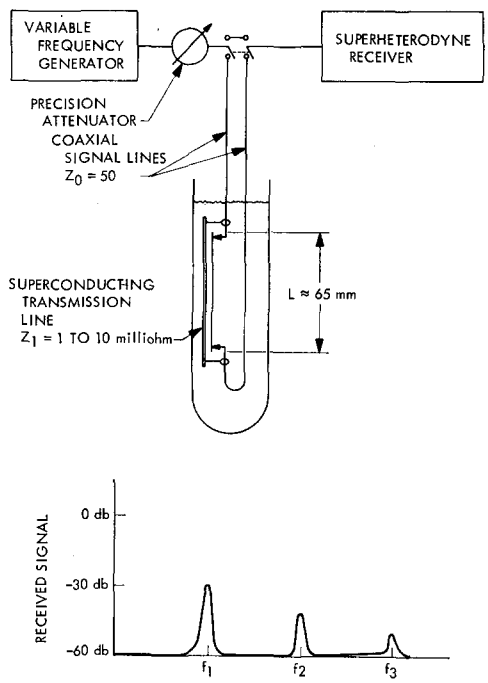

FIG. 6. Experimental apparatus and received signal.

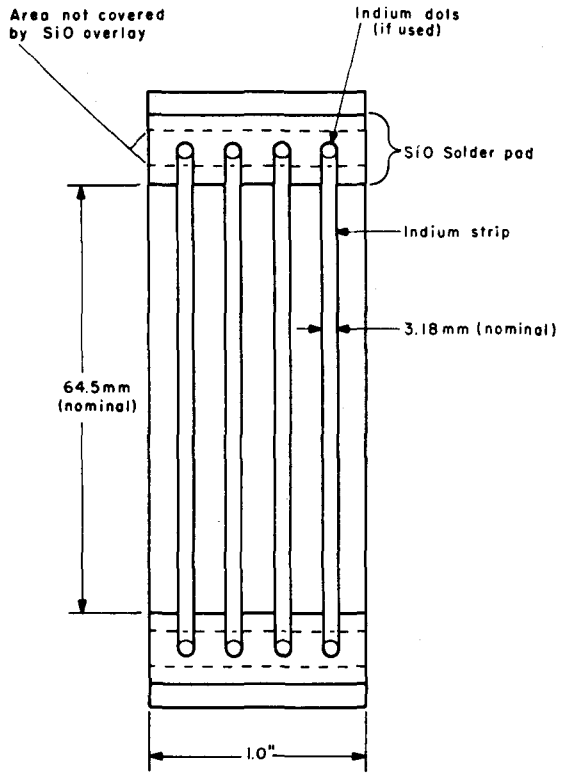

FIG. 7. Typical test sample.

Resistivity-heated tantalum boats held the charges to be evaporated. Masks to define evaporation geometry were carried on a rotating mask holder.

The final test strip is shown in Fig. 7. Four transmission lines were made on one strip. Silicon-monoxide[17] pads served to define the active length of the strip. The indium film[18] itself was evaporated, followed by an SiO overlay to prevent oxidation and to provide mechanical protection.

After preparation, the test strip was fastened in a test fixture. Input and output 50-Ω coaxial cables were clamped to the tantalum by a grounding strap soldered to the cable shield. The center conductor was connected to the film with a fine wire soldered with indium. The dc resistance and the 1-KHz capacitance were measured at 293°, 77°, and 4.2°K.

Resistance of a test slide was monitored during evaporation of the indium, and its thickness measured afterward using Tolansky multiple-beam interferometry.[19] Estimated accuracy of thickness measurements was ±20 A for 400 Å films up to ±50 Å for 5000 Å films. Width and length of the film were measured on a microscope with a vernier mechanical stage to an estimated accuracy of 0.1 mm.

[14] W. J. Tegart, *The Electrolytic and Chemical Polishing of Metals* (Pergamon Press, Inc., New York, 1959), p. 68.
[15] A. Charlesby and J. J. Polling, Proc. Roy. Soc. (London) **A227**, 434 (1955).
[16] L. Young, Proc. Roy. Soc. (London) **A244**, 41 (1958).
[17] Kemet Co., select grade.
[18] Johnson–Matthey, 99.99% pure indium.
[19] S. Tolansky, *Multiple Beam Interferometry of Surfaces and Films* (Clarendon Press, Oxford, 1968).

TABLE I. Estimates of λ_{In} from temperature dependence of velocity.

Assumed λ_{Ta}, Å	London			BCS Specular, $\xi_0=5.4\lambda_\infty$		
	$\langle\lambda_{In}\rangle$	$\langle\sigma_{LS}\rangle$	σ_λ	$\langle\lambda_{In}\rangle$	$\langle\sigma_{LS}\rangle$	σ_λ
400	730	27	143	685	19.1	128
500	717	22	128	...	...	...
580[a]	704	18.6	120	648	13.6	132
700	679	16.3	115	...	...	...
800	655	16.1	115	595	16.0	147

[a] Best estimate of λ_{Ta} from thickness data.

In order to obtain c_D it was necessary to measure the permittivity ϵ_D of the dielectric. This was done in two ways: first, by measuring the capacitance at 4.2°K; second, by extrapolating measured values of $(c_D/v_\phi)^2$ to infinite d. Agreement was good, the value of ϵ_D at 4.2°K being 21.5±0.3, yielding a best estimate of $c_D=0.216c$ or 6.43×10^7 m/sec.

IV. EXPERIMENTAL RESULTS AND ANALYSIS OF DATA

A. Velocity

1. Temperature Effects

In Fig. 8 we show typical results for fast, slow, and intermediate velocity films. The expected rapid decrease of v_ϕ as we approach T_c is found, as well as approach to a constant value when T is less than about 3°K.

The lower curve shown, film 31, exhibits the greatest slowing observed, amounting to $0.113c_D$. Since c_D itself is only $0.216c$, the total reduction is to $0.0243c$.

We wish to estimate λ_{In} and λ_{Ta}, the bulk penetration depths. We make use of Eq. (4), noting that τ_2 is effectively infinite. Also, we assume Gorter–Casimir temperature dependence[20]

$$\lambda(T)=\lambda(0)/[1-(T/T_C)^4]^{1/2}. \quad (10)$$

Since tantalum has a critical temperature of 4.38°K, compared with indium's 3.40°K, the former contributes no more than 10% of the change in $(c_D/v_\phi)^2$, and a correction may be made knowing λ_{Ta} only roughly. From thickness-dependence data, we arrived at $\lambda_{Ta}=$ 580 Å, and this value was used in making corrections.

For a London superconductor we may combine Eqs. (4), (6), and (10) to obtain

$$\lambda_{In}(T)\coth[\tau/\lambda_{In}(T)]=d(c_D/v_\phi)^2-d -\lambda_{Ta}(0)/[1-(T/4.38)^4]^{1/2}. \quad (11)$$

Using a computer, one may then solve for $\lambda_{In}(T)$ at each temperature. If we then assume that Eq. (10) holds, we can solve for $\lambda_{In}(0)$ and $T_c(\text{In})$, using Lock's method.[21]

A similar method can be used for other specular and diffuse cases, although the relationship expressed by Eq. (11) is known only numerically.

The results for several assumed values of λ_{Ta} and for two theories are given in Table I. The average values for all films tested and associated standard deviations are given. A standard deviation was calculated for the fit of Eq. (11) (or its numerical equivalent) to each individual film, in order to estimate the goodness of fit. The quantity $\langle\sigma_{LS}\rangle$ is the average of these. σ_λ is the standard deviation of the estimates of λ_{In}, and hence

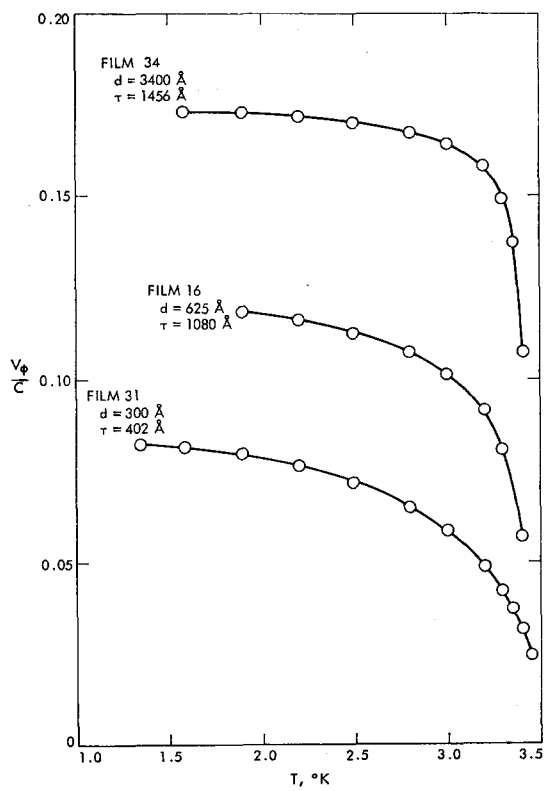

FIG. 8. Experimental temperature dependence of velocity.

[20] The BCS dependence differs slightly from this expression but made no significant difference in estimates of λ.

[21] J. M. Lock, Proc. Roy. Soc. (London) **A208**, 391 (1951).

measures the over-all experimental uncertainty of the given value of λ.

The specular case with $\lambda_{Ta}=580$ Å is seen to give significantly better fit to individual films, as is evidenced by the low value of $\langle\sigma_{LS}\rangle$. This agrees with the result of the analysis of the thickness data in the next section, where we find an average $\lambda_{Ta}=580$ Å and indications of some degree of specular reflection.

We thus conclude that the best estimate for λ_{In} is 648 ± 132 Å. We further conclude that the relationships expressed by Eq. (10) and the specular thickness dependence provide a good description of the temperature dependence of λ_{In}.

The calculated values of T_c thickness are plotted in Fig. 9. The solid line is from a calculation made by Toxen[12] which takes account of strains caused by differential thermal expansion of the indium and the substrate. He found $T_c(\infty)=3.408°K$, and our data bear this out.

2. *Thickness Effects*

In order to analyze effects of thickness, we have extrapolated all data to zero temperature by fitting an expression of the form

$$(c_D/v_\phi)^2=1+\frac{\lambda_{Ta}(0)}{[1-(T/4.38)^4]^{1/2}}+\frac{\lambda_{In}(0)}{[1-(T/T_c)^4]^{1/2}}. \quad (12)$$

The results for all films tested are shown in Fig. 10. All results for a given experimentally determined value of d have the same symbol. The heavy curve is a best fit of the London case, with the values of λ_{Ta} and λ_{In} adjusted to those shown. The dotted line is calculated from the specular theory using these same values. Our estimate $\lambda_{Ta}=580$ Å is taken from the weighted average

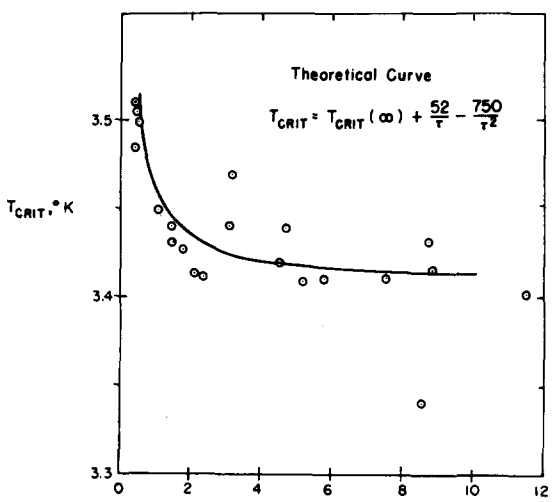

FIG. 9. Critical temperature dependence on thickness of indium film.

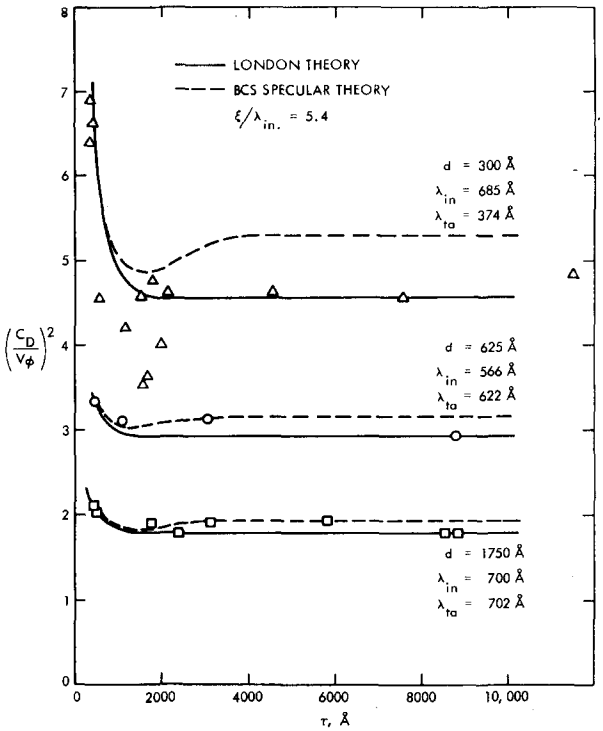

FIG. 10. Experimental dependence of velocity on film thickness with interfilm spacing as a parameter.

of the values given here. Since the data for $d=300$ Å are most sensitive to the external parameters, they are replotted in Fig. 11 to show the effects of choice of theory. In each case, λ_∞ and ξ_0 were chosen for best fit. The specular case, curves 4 and 5, provides the best fit to the dip in the data, while the diffuse case has the most rapid rise. However, none of the cases provide good fit over the entire range of data. We should like to have data for smaller τ_{In}, but the films here are the thinnest that could be made continuous because of agglomeration of the indium during deposition. The best we are able to conclude is that there seems to be some degree of specular reflection.

In view of the scatter of the data and lack of good fit, we cannot make a very precise estimate of λ_{In} and ξ_0. The data plotted in Fig. 11 are consistent with the estimate from temperature data of $\lambda=648\pm130$ Å for the London and specular cases. The diffuse case for $\lambda_\infty=300$ Å and $\xi_0=3000$ Å best fits the data, while that with $\lambda_\infty=600$ Å and $\xi_0=3240$ Å gives the rapid rise, but at a thickness of 700 Å instead of 450.

As we see from Eq. (4), a plot of $(c_D/v_\phi)^2$ vs $1/d$ should be linear with a vertical intercept of unity. The data of Fig. 10 are replotted thus in Fig. 12, using a value of $(c/c_D)^2=21.5$ obtained from capacitance data. The fit is reasonably accurate, especially for small τ. The intercept is quite close to unity, indicating excellent agreement between capacitance data and large d velocity measurements.

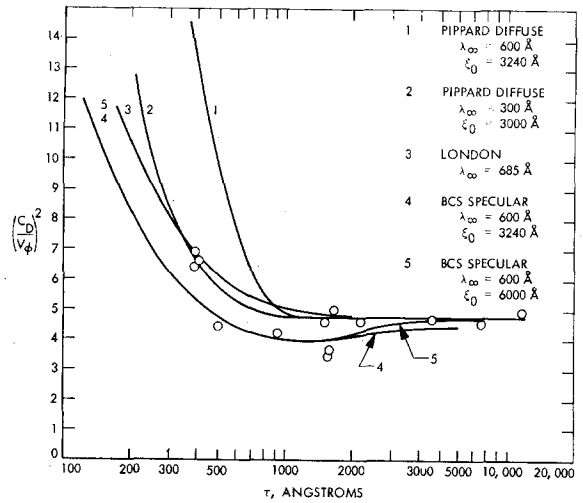

FIG. 11. Thickness dependence of penetration depth for $d=300$ Å compared with various theories.

3. *Frequency Effects*

Velocity was measured at higher harmonics for a number of films. Differences over the frequency range from 100 to 500 MHz were less than 1% in all but one film, for which they were less than 5%. We believe that the latter resulted from small irregularities in the film which caused frequency-dependent reflections.

B. Losses

1. *Temperature Effects*

From transmission-line theory we can predict that the Q of a transmission line, loaded as in Fig. 6, is given by

$$Q_n=[(L/n\pi)(R_{\text{surf}}/2Z_0)+(4/n\pi)(Z_0/Z_1)]^{-1}. \quad (13)$$

Here, R_{surf} is surface resistance per unit length, n is mode number, and the other parameters are defined in Fig. 6. The second term is negligible, being no more than 5% of the first at the highest Q's observed. Hence $1/nQ$ should be a direct measure of

$$R_{\text{surf}}=R_{\text{surf}}(\text{In})+R_{\text{surf}}(\text{Ta}). \quad (14)$$

Pippard[22] proposed the following empirical expressions for surface resistance:

$$R_{\text{surf}}=\text{Const}\, f^2t^4(1-t^2)/(1-t^4)^2, \quad (15)$$

where $t=T/T_C$. An analysis based on the BCS theory by Miller[23] justified this for $f<10$ GHZ and $0.4<t<0.8$.

Unfortunately, the effects of the indium and the tantalum, based on Eq. (15), overlap to such a degree that no separation seems feasible. Also, the Q's varied erratically from film to film with no discernible dependence on τ and d. Data for three films representing the extremes and a typical film are plotted in Fig. 13. The Q values for a number of films at two different temperatures are also given in Table II. It seems clear that wide variations between films result from slight variations in film preparation, an effect found by many experimenters. It is also clear that Q's are very low near T_C; in fact, this behavior sets the limit on how close to T_C we can make measurements.

In order to carry out measurements on the effects of temperature, one should form transmission lines of identical superconductors. Until this can be done we do not feel it worthwhile to examine the temperature dependence in detail.

2. *Frequency Effects*

Data on one film were taken over three octaves in frequency, and on a number of others over one octave. The results are plotted in Fig. 14, and compared to the line $R_{\text{surf}}\sim f^2$. With two exceptions the data tend parallel along this line, lending strong support to the $R_{\text{surf}}\sim f^2$ hypothesis.

C. Pulse Response

Since the application of superconducting transmission lines is most likely to be in the manipulation and

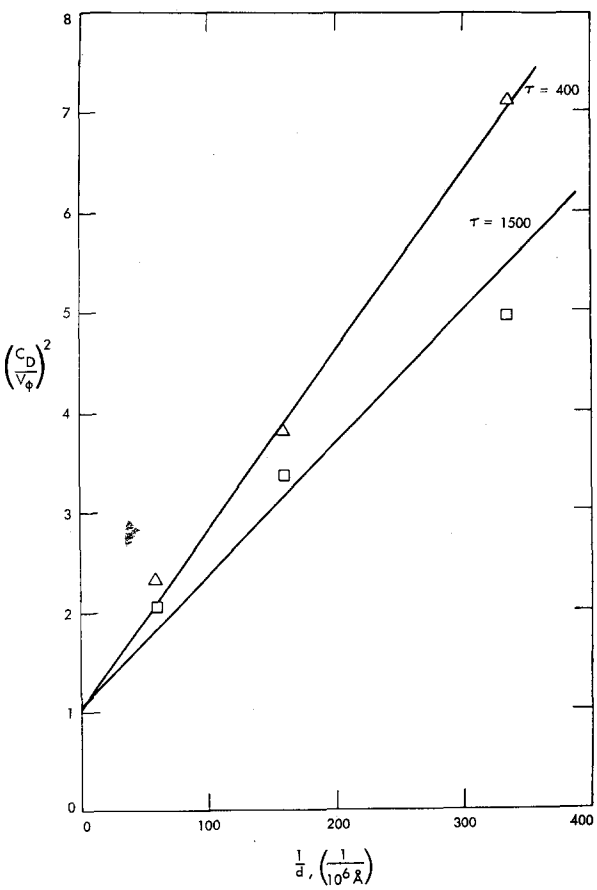

FIG. 12. Dependence of penetration depth on inverse film spacing.

[22] A. B. Pippard, Proc. Roy. Soc. (London) **A203**, 98 (1950).
[23] P. B. Miller, Phys. Rev. **118**, 928 (1960).

storage of pulses, it is of interest to examine the response to them. The signal generator and receiver of Fig. 6 are replaced by a mercury delay-line pulse generator and a sampling oscilloscope. Because of the severe mismatch between the coaxial signal lines and the superconducting line, the signal will suffer attenuation in passing onto the line, but once there it will be trapped by nearly perfect reflection at each end. The oscilloscope will see the pulse every two transits (a distance of about 13 cm) as it arrives at the output end. In Fig. 15 we show the response of film 22. Trace *a* is the input pulse, attenuated by 1000. Trace *b* is the response, unattenuated, at 3.380°K, very close to T_C. The velocity is low, but the attenuation is large, particularly for high-frequency components, so the pulse is distorted and spread out quickly. Trace *c* shows the response at 1.586°K. Attenuation and distortion are unmeasurable, but the velocity is somewhat higher, forcing the peaks closer together.

In order to examine the low attenuation and distortion, the pulse was observed after 1 μsec, as shown in trace *d*. The pulse is attenuated by 50%, but the shape is unchanged. Part of the attenuation is caused by reflection at the ends. The reflection coefficient is

$$\Gamma = V(\text{reflected})/V(\text{incident})$$
$$= (Z_0 - Z_1)/(Z_0 + Z_1) \approx 1 - 1.95 \times 10^{-4} \quad (16)$$

and it accounts for about 25% of the reduction.

A summary of results for three samples is presented in Table III. Film 22 has large d and τ; film 27, small d and intermediate τ; and film 31 has small d and small τ.

As we expect, the velocity is highest for 22 and lowest for 31. Temperature reduction has the largest effect on 31. The quantity v_ϕ/c measures the absolute reduction in speed over a free-space transmission line; v_ϕ/c_D measures the effect of the superconductors.

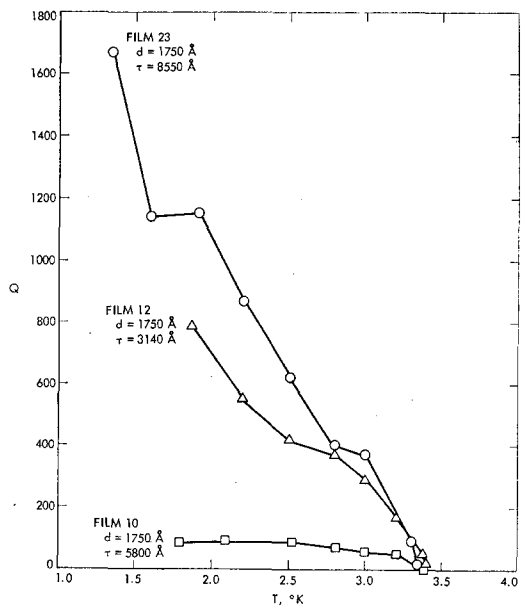

FIG. 13. Temperature dependence of resonance Q.

TABLE II. Q at two temperatures for a number of films.

Film	d	τ	$Q_{1.9}$	$Q_{0.985T_c}$
31	300	402	550	51
27	300	1 497	183	30
28	300	2 110	406	70
33	300	4 520	153	40
29	300	5 210	340	79
32	300	7 560	309	49
30	300	11 500	208	60
25	625	455	481	58
16	625	1 088	96	21
14	625	3 025	35	16.5
15	625	4 200	28	16.5
26	625	8 785	165	46
18	1755	413	265	31
13	1755	496	520	37
11	1755	1 140	52.5	16.5
9	1755	2 375	...	19
12	1755	3 140	770	45
10	1755	5 800	87	16
23.1	1755	8 548	1160	94
23.2	1755	8 548	1040	...
22	1755	8 844	960	63
34	3400	1 456	998	38

The attenuation α measures both the attenuation due to finite surface resistance and that due to imperfect reflections at each end. (Unfortunately, no delayed data were taken on 31, so no attenuation could be measured.) After removing the effect of reflections, we obtain α(intrinsic), which should be the attenuation on a long line.

Z_{char} is calculated by the formula

$$Z_{\text{char}} = (\mu_0/\epsilon_0)^{1/2}(d/W)(c_D^2/cv_\phi). \quad (17)$$

W is the width of the strip. Note that Z_{char} is increased by slowing due to the superconductor (c_D/v_ϕ) but decreased by that due to dielectric constant (c_D/c).

If we arbitrarily set 50% attenuation as the limit for a satisfactory line, we can calculate the longest permissible length and largest delay available. Furthermore, we estimate the pulse densities shown. These are pessimistic; the input pulse was about 2 nsec long and with shorter pulses the density could be much higher. All these figures together allow us to estimate the storage-capacity figures shown in the last line. It is

TABLE III. Pulse response of several transmission lines.

Film	22		27		31	
τ, Å	9000		1497		402	
d, Å	1750		300		300	
Temperature, °K	3.380	1.586	3.349	1.368	3.297	1.364
v_ϕ, cm/nsec	3.32	4.42	2.1	3.23	1.39	2.65
v_ϕ/c	0.111	0.147	0.070	0.107	0.0463	0.0883
v_ϕ/c_D	0.514	0.684	0.324	0.500	0.215	0.409
α/cm	0.0133	1.3×10^{-4}	0.0089	5.8×10^{-4}	0.0106	Unmeasurable
$\alpha_{\text{intrinsic}}$/cm	0.0133	1.00×10^{-4}	0.0089	5.8×10^{-4}	0.0106	...
Z_{char}, mΩ	6.80	4.87	2.15	1.39	3.43	1.81
Line length, cm 50% attenuation	51	6930	80	1180	60	Large
Delay, nsec for 50% attenuation	15.5	1570	37	356	43	...
Estimated permissible density of pulses/cm	>0.15	>0.15	>0.15	>0.3	>0.23	...
Estimated storage capacity, pulses	>8	>1040	>12	>350	>26	...

probable that these could be increased by at least a factor of 4 using shorter pulses, and by another factor of 4 by allowing attenuation to $\frac{1}{8}$ of the initial value.

We conclude that the choice of film thickness, interfilm spacing, and operating temperature depends on the application. If long delays are wanted, operation with small τ and d at high temperature (but not quite so close to T_C) is indicated. If a large number of pulses are to be stored, larger τ and d, and lower temperatures to reduce attenuation and distortion are indicated.

V. SUMMARY AND CONCLUSIONS

We have given theoretical calculations and experimental measurements of the dependence of phase velocity in a superconducting transmission line on film thickness, interfilm spacing, bulk penetration depth

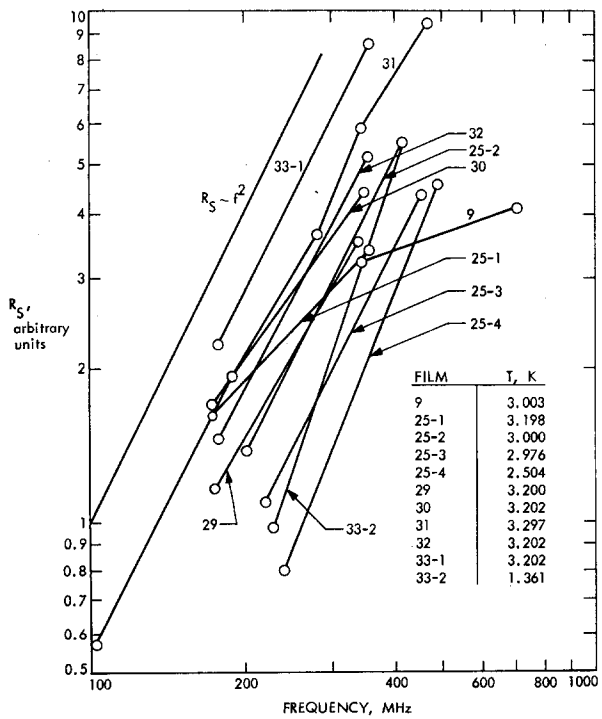

FIG. 14. Frequency dependence of surface resistance.

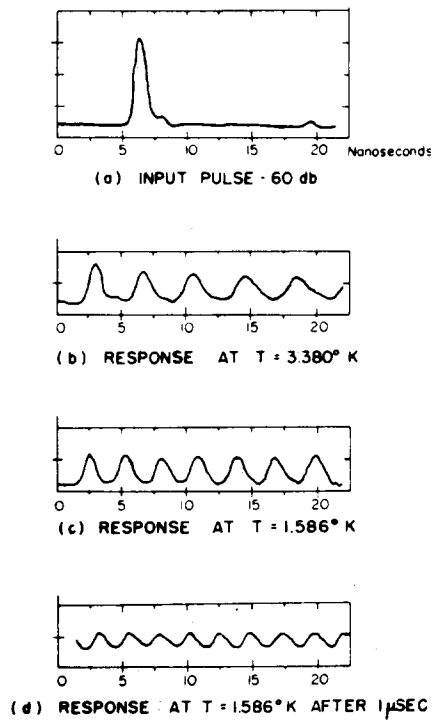

FIG. 15. Pulse response of film 22.

and on parameters such as temperature and magnetic field which affect the bulk penetration depth.

The theory predicts large reductions in velocity for thin, closely spaced films, for films measured near critical temperature, and for very impure films. It predicts qualitative differences in film thickness dependence between specular and diffuse reflection of electrons at the film surfaces.

Experiments show the expected dependences on temperature and geometry. Dependence on temperature shows small scatter and good agreement with predictions of the Gorter–Casimir two-fluid theory. It allows us to predict a bulk penetration depth for indium of 648 ± 132 Å, in good agreement with other results.

Dependence on geometry shows far more scatter, as a result of the fact that comparisons must be made between different films. We find the results consistent with $\lambda_{In}=648$ Å, $\xi_0\approx3240$ Å, and $\lambda_{Ta}=580$ Å, and we conclude that some degree of specular reflection is present.

Within our experimental error, velocity and hence surface reactance does not depend on frequency over the range 50–500 MHz. Attenuation and hence surface resistance appears to increase as the square of frequency, consistent with Miller's theory.[23]

Pulse measurements indicate that delays of several microseconds are feasible without undue attenuation and distortion. Storage of several thousand pulses on a single line fabricated by microcircuit techniques is feasible.

We conclude that the resonance technique is a precise tool for the study of effects which can be measured on a single film, i.e., temperature, magnetic field, and frequency dependence of penetration depth. However, for study of effects, such as thickness dependence, which depend on comparison between films, better techniques of preparation to insure more uniform films must be developed.

ACKNOWLEDGMENTS

The authors would like to thank the following persons: R. L. Carrouché, who constructed much of the necessary apparatus; J. B. Trenholme, who assisted with film fabrication and experimental measurements, and Marge Brandenberg, who assisted nobly in the preparation of the manuscript.

APPENDIX A: DEPENDENCE OF PHASE VELOCITY ON PENETRATION DEPTH

We wish to solve the boundary value problem of Fig. 1, where a dielectric slab separates two superconductors of penetration depths $\lambda_1(\tau_1)$ and $\lambda_2(\tau_2)$. The solution will express the phase velocity in terms of λ_1, λ_2, and d.

It is convenient to work with the surface impedance, which is defined for a material lying in the region $y>0$ by[24]

$$Z_s=E_{\tan}(0)/H_{\tan}(0). \tag{A1}$$

For a lossless superconductor, this can be related to the penetration depth defined in Eq. (2) by use of Maxwell's equations as

$$\lambda(\tau)=Z_s/j\omega\mu_0. \tag{A2}$$

For pure E-mode or pure H-mode solutions, it is sufficient to match Z_s across a boundary rather than $E_{\tan}$ and $H_{\tan}$ separately. Since Z_s is independent of coordinates, these may be chosen as convenient at each stage of the solution.

In the geometry of Fig. 1, we assume that Z_1 and Z_2 are the surface impedances of the upper and lower films. If we assume a slow-wave E-mode solution (i.e., $v_\phi<c_D$) propagating in the z direction, all fields vary as $\exp[j(\omega t-\beta z)]$; E_x, H_z, and $H_y=0$; and all field equations can be expressed in terms of E_z. We can then show that the longitudinal electric field in the dielectric is

$$E_z=A(\sinh\gamma y+B\cosh\gamma y). \tag{A3}$$

Here the propagation constant γ is real since

$$\gamma^2=\beta^2-\omega^2/c_D^2=\omega^2(v_\phi^{-2}-c_D^{-2}). \tag{A4}$$

It can be shown that

$$H_x=(-j\omega\epsilon_D/\gamma^2)(\partial E_z/\partial y), \tag{A5}$$

hence the surface impedance at any position in the dielectric is given by

$$Z_s(y)=E_z/H_x=j\gamma(\tanh\gamma y+B)/\omega\epsilon_D(1+B\tanh\gamma y). \tag{A6}$$

We apply the two boundary conditions[25]

$$Z_s(d)=Z_1 \tag{A7a}$$

$$Z_s(0)=-Z_2. \tag{A7b}$$

We eliminate B between the resulting equations,

$$j\gamma\tanh\gamma d=\omega\epsilon_D(Z_1+Z_2)+\omega^2\epsilon_D^2Z_1Z_2(\tanh\gamma d/j\gamma). \tag{A8}$$

The second term can be shown to be about 10^{-8} smaller than the first because the λ's and d are of the order of 10^{-4} wavelengths, and γ is of the order of a wavelength. Also since $\gamma d\ll1$, we have

$$j\gamma^2d\approx\omega\epsilon_D(Z_1+Z_2). \tag{A9}$$

Using Eqs. (A2), (A4), and the identity $c_D^2=1/\mu_0\epsilon_D$, we have

$$(c_D/v_\phi)^2=1+\lambda_1(\tau_1)/d+\lambda_2(\tau_2)/d. \tag{A10}$$

[24] The sign of Z_s is chosen to make it positive when power flows into a lossy material. For a material lying below $y=0$, Z_s is the negative of Eq. (A1).

[25] The negative sign arises because material 2 lies below $y=0$.

APPENDIX B: CALCULATION OF SURFACE IMPEDANCE OF A THIN FILM

A. London Superconductor

For a London superconductor in the quasistatic approximation and a transverse gauge ($\nabla\cdot A=0$), we have the electrodynamic equation

$$\nabla^2 E=E/\lambda_L^2, \tag{B1}$$

whose solution in one dimension with

$$E_z=E_z\exp[j(\omega t-\beta z)]$$

is

$$E_z=A(\sinh y/\lambda_L+B\cosh y/\lambda_L). \tag{B2}$$

Using Maxwell's equations to obtain H_x and assuming $\beta\lambda_L\ll 1$, we can show that

$$Z_s(y)=E_z/H_x=-j\omega\mu_0\lambda_L\left(\frac{\tanh y/\lambda_L+B}{1+B\tanh y/\lambda_L}\right). \tag{B3}$$

The result does not depend on choice of coordinate system. We assume that the slab faces free space at the surface $y=\tau$ and solve for Z_s at $y=0$. We can show that, for slow waves and for $\lambda_L\ll$(free-space wavelength), the surface impedance at the upper face is essentially infinite unless another superconductor lies within a few penetration depths. Hence, at $y=0$

$$Z_s\approx j\omega\mu_0\lambda_L\coth\tau/\lambda_L, \tag{B4}$$

which is equivalent to Eq. (6).

B. Specular Reflection of Electrons

We use a method similar to one developed by Schrieffer[11] modified to suit different boundary conditions. We express the relation between $\mathbf{J}_s$ and $\mathbf{A}$ in momentum space as

$$-\mu_0\mathbf{J}_s(\mathbf{k})=K(\mathbf{k})\mathbf{A}(\mathbf{k}). \tag{B5}$$

The kernel $K(k)$ is given for the three theories as

London

$$K_L(\mathbf{k})=1/\lambda_L^2; \tag{B6}$$

Pippard

$$K_P(\mathbf{k})=(1/\lambda_L^2)[6\pi/\xi_0\xi^2k^2][(1+(\xi k)^2)\tan^{-1}k-\xi k]; \tag{B7}$$

BCS

$$K_{\mathrm{BCS}}(\mathbf{k})=\tfrac{3}{4}(1/\lambda_L^2)(1/\xi_0 k)\ln(1+\xi k); \tag{B8}$$

where $k=|\mathbf{k}|$.

We wish to solve the problem with the boundary conditions $B_x=B_0$ on the lower surface and $B_x=0$ on the upper (equivalent to the infinite surface impedance of free space assumed in the London case). As discussed by Schrieffer, the specular boundary condition may be represented mathematically by solving an equivalent antisymmetric periodic problem in which each electron approaching a film surface is met by another with the same x and z momentum, but opposite y momentum.

We introduce fictitious current sheets as shown in Fig. 16 to obtain the necessary antisymmetric periodic B field. Note that at $y=0$, $B_x=B_0$, and at $y=\tau$, $B_x=0$, as required.

Applying a Fourier cosine transform with respect to y, we find that the currents may be represented by

$$\begin{aligned} k=0:&\quad \mathbf{J}_z^*(k)=B_0/\mu_0\tau \\ k\neq 0:&\quad =2B_0/\mu_0\tau. \end{aligned} \tag{B9}$$

The electrodynamic equation we wish to solve is, in discrete k space

$$\mathbf{k}_n^2 A_z(k_n)=\mu_0[J_s(\mathbf{k}_n)+J_z^*(\mathbf{k}_n)], \tag{B10}$$

where $\mathbf{k}_n=e_z n\pi/\tau$, and e_z is the z-directed unit vector.

Combining Eqs. (B5), (B9), and (B10), we have

$$\begin{aligned} &k=0,\quad 0=-A_z(0)K(0)+B_0/\tau \\ &k\neq 0,\quad k_n^2A_z(k_n)=-A_z(k_n)K(k_n)+2B_0/\tau. \end{aligned} \tag{B11}$$

Solving for A_z and forming the Fourier sum, we have

$$A_z(y)=B_0/\tau\{1/K(0)+2\sum_{n=1}^{\infty}\cos(k_n y)/[k_n^2+K(k_n)]\}. \tag{B12}$$

Using the equality valid in transverse gauge, $E=-j\omega A$, we have

$$\begin{aligned} \lambda(\tau)&=Z_s(0)/j\omega\mu_0=A_z(0)/B_0 \\ &=(1/\tau)\{1/K(0)+2\sum 1/[k_n^2+K(k_n)]\}. \end{aligned} \tag{B13}$$

For the London case we insert (B6) and sum the series analytically, obtaining Eq. (B4). For the Pippard and BCS cases, the summation must be done numerically.

C. Diffuse Reflection of Electrons

The requirement that reflection be diffuse is equivalent to the condition that the electrons crossing the

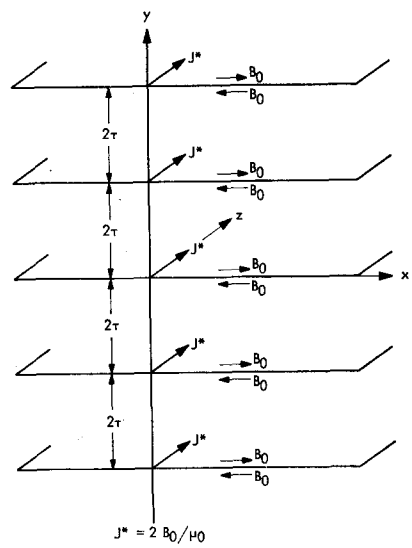

FIG. 16. Equivalent current sheets to simulate specular reflection of electrons.

surface from outside the film come from a field-free region and therefore have a random velocity distribution. As Schrieffer shows, this leads to the following equation for vector potential (rewritten in our coordinate system, and for boundaries at 0 and τ)

$$d^2A_z(y)/dy^2=\int_0^\tau G(y-y')A_z(y')dy', \quad \text{(B14)}$$

where $G(y-y')$ is as defined by Schrieffer. For a Pippard superconductor, G is given by

$$G(y-y')=(3/4\xi_0\lambda_L^2)$$
$$\times[-Ei(-x)(1-x^2/2)-(e^{-x}/2x^2)(1-x)], \quad \text{(B15)}$$

where $x=|y-y'|/\xi_0$ and $-Ei(-x)$ is the exponential integral.

We can show that

$$Z_s=-j\omega\mu_0A_z/A_z'. \quad \text{(B16)}$$

We now assume that the surface impedance at one surface, say the lower, is infinite so that $A_z'(0)=0$ We set $A_z(0)=1$, then use Eq. (B14) to find $A_z(\tau)$ and $A_z'(\tau)$. Integration gives us

$$A_z'(y)=\int_0^\tau\int_0^y A_z(y')G(t-y')dtdy'. \quad \text{(B17)}$$

Then integration by parts gives

$$A_z(y)=1+\int_0^\tau A_z(y')\left(\int_0^y (y-t)G(t-y')dt\right)dy'. \quad \text{(B18)}$$

We solve this numerically as follows. Let

$$H(y,y')=\int_0^y (y-t)G(t-y')dt. \quad \text{(B19)}$$

This is calculated by Simpson's rule integration. Then an n-interval Simpson's rule integration of Eq. (B18) gives the value of $A_z(y)$ at the $n+1$ evenly spaced points from 0 to τ as

$$A_z(l\tau/n)=1+(\tau/3n)\sum_{i=0}^{n} A_z(i\tau/n)H[(l\tau/n),(i\tau/n)],$$
$$l=0,1,2,\cdots,n. \quad \text{(B20)}$$

Since we have now $n+1$ equations in $n+1$ unknows, we may solve for the $A(0),\cdots,A(\tau)$. Equation (B17) is then integrated numerically to obtain $A_z'(\tau)$, and (B16) is used to obtain $Z_s(\tau)$.

The principal calculational difficulty is that $G(t-y')$ approaches a Dirac delta function as $\xi_0\to 0$.[26] In order to calculate the $(n+1)^2$ values of H in reasonable time, it is necessary to write a Simpson's rule program which varies the interval of integration, using a fine interval only in the region where required for accuracy.

[26] In fact, it can be shown to become $\lambda_L^{-2}\delta(t-y')$. Equation (B14) then has the solution

$$A_z(y)=\cosh y/\lambda_L \quad \text{and} \quad Z_s(t)=-j\omega\mu_0\lambda_L\coth y/\lambda_L,$$

the London value given by Eq. (B4). The negative sign arises because we are computing Z_s at the upper face.

JOURNAL OF APPLIED PHYSICS VOLUME 40, NUMBER 5 APRIL 1969

Additional Papers Given in This Session

Tuning Superconducting Microwave Cavities*

T. I. SMITH

W. W. Hansen Laboratories, Stanford University, Stanford, California 94305

The extremely high Q of superconducting microwave cavities makes them very attractive for use in many applications. In some of these applications the resonant frequency of the superconducting cavity must be adjustable while the cavity is at liquid-helium temperatures. Because of the requirement that the losses in the tuning mechanism be very low, in order that the Q of the cavity not be degraded, the usual methods of tuning microwave cavities are not always applicable to superconducting devices. One example of a case in which new techniques have had to be developed is the superconducting linear accelerator which is being constructed at Stanford University. In this accelerator, 25 superconducting sections, each 20 ft long, will have to resonate at the same frequency to within about 1 part in 10^3. The sections are being constructed to be tunable at liquid-helium temperatures over a range of 1 part in 10^4, with a resolution of 1 part in 10^4.

* Work supported in part by the U.S. Office of Naval Research, Contract [Nonr 225(67)].

Multiresonator Superconducting Band-Pass and Band-Reject Filters

F. ARAMS, R. DOMCHICK, K. SIEGEL, R. SLEVEN, J. TAUB, AND N. WORONTZOFF

Airborne Instruments Laboratory, Division of Cutler-Hammer, Melville, L. I., New York 11746